Available online at www.sciencedirect.com
ScienceDirect
Carbon 45 (2007) 1606–1613
CARBON
www.elsevier.com/locate/carbon

Analytical model of piezoresistivity for strain sensing in carbon fiber polymer–matrix structural composite under flexure

Sirong Zhu [1], D.D.L. Chung *

Composite Materials Research Laboratory, University at Buffalo, State University of New York, Buffalo, NY 14260-4400, USA

Received 4 January 2007; accepted 6 April 2007
Available online 19 April 2007

Abstract

An analytical model is provided for the piezoresistive phenomenon of continuous carbon fiber polymer–matrix composite under flexure. This phenomenon allows strain sensing and entails reversible increase of the tension surface resistance and reversible decrease of the compression surface resistance during flexure. The model considers the surface resistance change to be due to change in the degree of current penetration. The longitudinal strain resulting from the flexure affects the through-thickness resistivity (which relates to the contact resistivity of the interlaminar interface). Good agreement is found between the model and prior experimental results, except that the calculated surface resistance on the tension side is higher than the measured value, when the magnitude of the average longitudinal strain on the surface exceeds 3×10^{-3}.
© 2007 Elsevier Ltd. All rights reserved.

1. Introduction

Polymer–matrix composites with continuous carbon fiber reinforcement are the dominant advanced lightweight structural materials, due to their combination of high strength, high modulus of elasticity and low density. Their extent of usage in aircraft structural components has been increasingly significantly in recent years. Usage in automobile structural components has started. In addition, these composites are used in a large variety of sporting goods.

Vibration reduction is needed for most structures, due to the resulting improvement in performance, control and safety. Associated with vibration reduction is the sensing of vibration, which relates to the sensing of strain. In the elastic regime, stress and strain are proportional to one another. Thus, strain sensing relates to stress sensing, which in turn relates to load monitoring. The monitoring of the load is valuable for operation control. Moreover, the monitoring of the load history is useful for determining the cause of damage of a structure.

The sensing of strain is conventionally attained by the use of attached or embedded strain sensors, such as metal films that change in dimensions, and hence, in electrical resistance in response to strain. Strain sensing can also be attained by the use of embedded fiber-optic sensors. These methods suffer from the cost and low durability of the sensors. In the case of embedded sensors, additional problems relate to the low maintainability and the possible decrease in the mechanical performance due to the presence of the embedded sensors.

An emerging and attractive method of strain sensing involves using the structural material itself as the sensor [1,2]. This means that there is no attached or embedded sensor. This method is known as self-sensing and is attractive because of its low cost, high durability, large sensing volume and absence of mechanical property loss. The ability of structural materials to sense their own strain has been reported in carbon fiber (continuous) polymer–matrix composites [3,4] and in carbon fiber (discontinuous) cement–matrix composites [5–7]. The self-sensing ability in these composites is based on piezoresistivity, which is the

* Corresponding author. Fax: +1 716 645 3875.
E-mail address: ddlchung@buffalo.edu (D.D.L. Chung).
URL: http://alum.mit.edu/www/ddlchung (D.D.L. Chung).
[1] Permanent address: Department of Engineering Structures and Mechanics, School of Science, Wuhan University of Technology, Wuhan, Hubei 430070, China.

0008-6223/$ - see front matter © 2007 Elsevier Ltd. All rights reserved.
doi:10.1016/j.carbon.2007.04.012

phenomenon in which the electrical resistivity of the material changes reversibly with strain. In contrast, the metal film strain gages are not based on piezoresistivity, since the resistivity of the metal does not change with strain. The fact that the resistivity changes with strain enhances the effect of strain on the electrical resistance, thereby resulting in high sensitivity.

A figure of merit for sensors that are based on changes in the electrical resistance is the gage factor, which is defined as the fractional change in resistance per unit strain. When the resistivity does not change with strain, the gage factor is around two; the exact value depends on the Poisson ratio. For example, a carbon–matrix composite with continuous carbon fibers has a gage factor of two [8]. When the resistivity changes with strain, the gage factor can be higher than two by one or two orders of magnitude. In the case of epoxy–matrix composites with continuous carbon fibers, the gage factor is as high as 49 [9]. The high value of the gage factor for the epoxy–matrix composite is due to the large difference in electrical resistivity between the carbon fiber and the polymer matrix and the consequent large effect of strain-induced microstructural changes on the electrical resistivity of the composite. An example of a microstructural change is the change in the extent of fiber–fiber contact across the interlaminar interface, i.e., the interface between adjacent laminae in the composite. Upon application of a compressive stress in the direction perpendicular to the laminae, the extent of fiber–fiber contact across the interlaminar interface of a carbon fiber epoxy–matrix composite increases, thereby causing decrease in the contact electrical resistivity associated with the interlaminar interface [10]. This contact resistivity is never infinity, due to the presence of fiber–fiber contacts, which are due to the fiber waviness and the imperfect coverage of the fibers by the epoxy resin during composite fabrication. In a carbon–carbon composite, the carbon fiber and carbon matrix are similar in resistivity, so strain-induced microstructural changes have relatively little effect on the electrical resistivity of the composite and the gage factor is low [8].

Flexure is a common manner of loading of structures, particularly composite panels. It is more commonly encountered in composite structures than uniaxial tension or uniaxial compression. For example, a bird hitting a wing of an aircraft results in flexural loading. Under flexure, one side is under tension, while the opposite side is under compression. For an epoxy–matrix composite with continuous carbon fibers in the quasi-isotropic lay-up configuration, the DC electrical resistance of the tension surface increases reversibly upon flexure, while that of the compression surface decreases reversibly [11]. The surface resistance is to be distinguished from the volume resistance. The surface resistance is measured using electrical contacts that are all on the same surface (the same side) of the specimen. The penetration of the surface current into the interior is limited, because the fibers are in the plane of the laminate and the resistivity of the composite is much higher in the through-thickness direction than the longitudinal direction. On the other hand, the volume resistance is measured using electrical contacts that are designed to provide current penetration throughout the entire cross-section of the specimen. The relatively large change in the surface resistance during flexure is attributed to the decrease in the degree of current penetration at the tension side upon flexure and the increase in the degree of current penetration at the compression side upon flexure [11]. That the current penetration decreases at the tension surface is consistent with the report that the through-thickness resistivity increases during uniaxial tension [9,11,12]. During uniaxial tension, the fractional change in the longitudinal volume resistance is small compared to the fractional change in the through-thickness resistance [11].

In spite of the detailed experimental results reported for the piezoresistive behavior of a quasi-isotropic carbon fiber epoxy–matrix composite under flexure [11], no model has been presented to explain the behavior. The modeling that has been reported previously is limited to a laminate theory that is aimed at calculating the piezoresistive behavior in various directions of the composite [13] and a finite element model of the current flow in a unidirectional carbon fiber composite [4].

Although damage sensing is important and the electrical resistance can be used to indicate damage [14–22], this paper addresses the effect of strain rather than the effect of damage. The scientific origin of damage is quite different from that of strain. Damage involves delamination and fiber breakage that are irreversible. In contrast, strain involves subtle microstructural changes that are reversible. Models have been reported in prior work to relate the electrical resistivity of continuous carbon fiber polymer–matrix composites to the damage [3] and to the damage distribution [23,24].

This paper is aimed at providing an analytical model for the piezoresistivity in continuous carbon fiber epoxy–matrix composite under flexure. The piezoresistivity is in relation to strain rather than damage. The model allows better understanding of the origin of the piezoresistivity. In addition, it will be useful for calculation of the piezoresistive effect for structures of various shapes, as encountered in practical implementation of the strain self-sensing technology.

2. Modeling the surface electrical resistance

The modeling of the electrical resistance is necessary for modeling the piezoresistive behavior, since the resistance is the quantity measured in the piezoresistivity experiment. The utilization of the piezoresistivity under flexure involves measurement of the surface resistance [11], which is measured by using electrical contacts that are on one surface of a specimen; the surface is in the plane of the laminate.

As illustrated in Fig. 1, the specimen is under three-point bending with a span of 80 mm [11]. Contacts A_1, B_1, C_1 and D_1 allow measurement of the top surface resistance

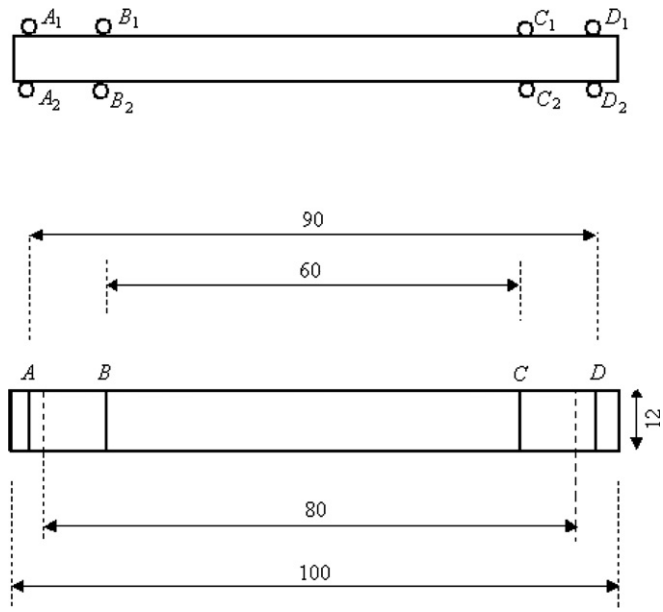

Fig. 1. Schematic of the edge of a composite to illustrate the concept behind the placement of electrical contacts. A_1, B_1, C_1, and D_1 are contacts on one surface; A_2, B_2, C_2 and D_2 are contacts on the opposite surface. All the electrical contacts are strips of about 2 mm wide oriented in the direction perpendicular to the length of the composite [11]. All dimensions are in mm.

using the four-probe method; contacts A_2, B_2, C_2 and D_2 allow measurement of the bottom surface resistance. The tension surface resistance was measured by using A_2 and D_2 as current contacts and B_2 and C_2 as voltage contacts. The compression surface resistance was measured by using A_1 and D_1 as current contacts and B_1 and C_1 as voltage contacts.

The current contacts (A and D, 90 mm apart [11]) allow the current to be injected from one surface, rather than being injected uniformly throughout the cross-section of the specimen. The voltage contacts (C and D, 60 mm apart [11]) allow the voltage to be measured on the surface. Thus, the surface resistance, as obtained by dividing the voltage between the surface voltage contacts by the current injected by the surface current contacts, is to be distinguished from the volume resistance, which is ideally measured by using current contacts that allow uniform current injection throughout the cross-section. Due to the assumed uniformity of the current density in the cross-section of the specimen in the case of volume resistance measurement, the volume resistance is simply related to the volume electrical resistivity of the specimen. However, due to the non-uniformity in the current density in the case of surface resistance measurement, the surface resistance is not simply related to the volume resistivity.

The laminate consists of n laminae ($n = 24$ [11]) that are labeled i, where $i = 1, 2, \ldots, n$. Let the length and width of the laminate be L and b, respectively. Let the thickness of the ith lamina be $t(i)$. These dimensions are parameters in the model. The effect of topography may be treated by the use of different dimensions for various parts of a composite component.

The thickness $t(i)$ increases with the number of fibers in a tow used in the composite fabrication. It also increases with the matrix volume fraction of the matrix in the composite. The volume fraction of matrix is typically low (around 40%) in a continuous carbon fiber polymer–matrix structural composite, so it does not tend to vary significantly. On the other hand, non-uniformity in the matrix distribution may occur in a composite due to non-ideal composite fabrication conditions. The non-uniformity may be modeled by using different values of t for various laminae in the composite, or by using different values of t for different regions of the same lamina. The effect of such non-uniformity is not explicitly addressed in this paper. The experimental results [11] used in this paper for comparing with the modeling results were obtained on a commercially made composite with good fiber distribution, and hence little, if any, resin rich regions.

The electrical conduction of the composite in the fiber direction is due to the electrical conduction of fibers. The conduction in the through-thickness direction is due to the fiber–fiber contacts across the interlaminar interface, as well as the contacts between fibers within the same lamina. The fiber–fiber contacts within a lamina are expected to be more abundant than those across an interlaminar interface, since the interface is a region, where the fibers are not as densely packed [10].

Different polymer matrices are associated with different extents of flow of the resin during composite fabrication. Thus, a change in the polymer matrix can affect the extent of fiber–fiber contact across the interlaminar interface, thereby affecting the piezoresistive behavior of the composite. A change in the matrix volume fraction has similar effects. The effects of the matrix type and of the matrix volume fraction are not treated in this paper.

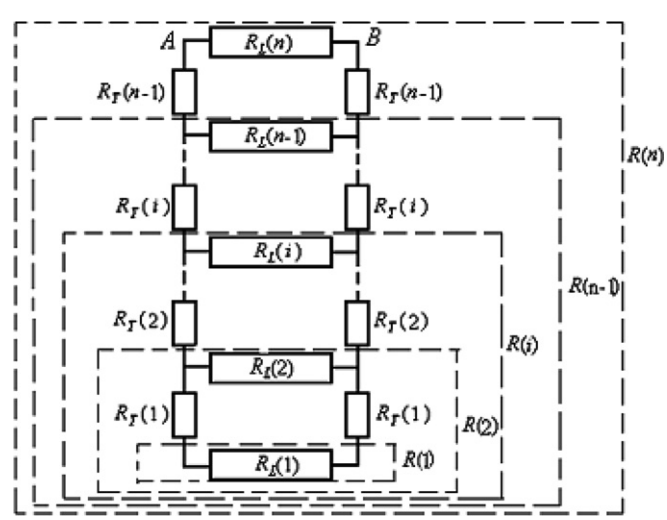

Fig. 2. Equivalent electrical circuit used for calculating the surface resistance. The surface is at the top of the diagram.

In order to calculate the total change in resistance ΔR, we use an equivalent electrical circuit to describe the beam, as shown in Fig. 2. $R_L(i)$, the longitudinal resistance of the ith lamina, is associated with an element of length L_c (the distance between the two voltage contacts, B and C, as shown in Fig. 1), thickness $t(i)$ and width b. Hence

$$R_L(i) = \frac{\rho_L(i)L_c}{t(i)b}, \quad (1)$$

where $\rho_L(i)$ is the volume electrical resistivity of lamina i in the longitudinal (0°) direction. Different plies can have different values of ρ_L, due to the difference in fiber direction. The fiber volume fraction of the composite will affect $\rho_L(i)$, in addition to affecting the extent of fiber–fiber contact across the interlaminar interface.

Let $R_T(i)$ be the through-thickness resistance associated with half of the i th lamina. This means that the resistance associated with each lamina is contributed by $R_L(i)$ and two of $R_T(i)$, as shown in Fig. 2. As explained earlier, $R_T(i)$ is assumed to be dominated by the contact resistance of the interlaminar interface between the ith and $(i-1)$th laminae. Let the contact resistivity of this interface be $\rho_T(i)$. Since the contact resistance of an area is equal to the contact resistivity multiplied by the area

$$R_T(i) = \frac{2\rho_T(i)t(i)}{L_c b}, \quad (2)$$

where $\rho_T(i)$ is the through-thickness resistivity that reflects the fiber–fiber contacts within a lamina and those across an interlaminar interface.

The top surface resistance $R(n)$, i.e., the resistance measured between the two terminals of resistor $R_L(n)$, as shown in Fig. 2, is calculated by considering this surface resistance to be $R_L(n)$ in parallel with the sum of $R_T(n-1)$, $R_L(n-1)$ and $R_T(n-1)$, which are in series, as shown in Fig. 2. In general, the resistance $R(i)$ between the two terminals of $R_L(i)$ is obtained by considering $R_L(i)$ in parallel with the sum of $R_T(i-1)$, $R_L(i-1)$ and $R_T(i-1)$. In other words

$$R(1) = R_L(1), \quad (3)$$

$$R(i) = \frac{(2R_T(i-1) + R(i-1))R_L(i)}{R_L(i) + 2R_T(i-1) + R(i-1)} \quad (i = 1, \ldots, n) \quad (4)$$

and

$$R(n) = \frac{(2R_T(n-1) + R(n-1))R_L(n)}{R_L(n) + 2R_T(n-1) + R(n-1)}. \quad (5)$$

The composite is a commercially manufactured 24-lamina quasi-isotropic $[0/45/90/-45]_{3s}$ laminate of size $100 \times 12 \times 3.2$ mm. For details on the composite constituents and the measurement methods, please refer to Ref. [11]. The measured surface resistance $R(n)$ is 2.5257 Ω [11]. The measured values of the electrical resistivity are 0.007 and 600 Ω cm in the longitudinal and through-thickness directions, respectively [25]. Thus, the composite is highly anisotropic, with the ratio of the two resistivities being 10^5. Our model assumes that the longitudinal resistivity of a lamina in the 0° direction is $\rho_L(1) = 0.0076$ Ω cm, and that both the longitudinal resistivity of a 45, 90 or −45° lamina and the through-thickness resistivity are 650 Ω cm. These values are close to the measured values of the longitudinal and through-thickness resistivity for this composite [11]. The transverse resistivity in the 90° direction is comparable to the through-thickness resistivity, as shown in prior work on a unidirectional composite [26]. The resistivity in the ±45° direction is actually lower than that in the 90° direction, but both are much higher than that in the 0° direction, due to the need for the associated current to cross the polymer matrix that separates adjacent fibers. Thus, in this model, we assume that the longitudinal resistivity is similarly high for the ±45° and 90° laminae.

3. Modeling the piezoresistivity

In the electrical model of Fig. 2, there are the longitudinal resistance and the through-thickness resistance. Upon loading, both resistances can change. It is assumed that the change in through-thickness resistance (primarily the contact resistance between adjacent laminae) is responsible for the piezoresistive effect under flexure. This assumption is consistent with the experimental observation that: (i) the through-thickness resistivity decreases upon longitudinal uniaxial tension [9,11,12], (ii) the effect of longitudinal uniaxial tension on the longitudinal volume resistivity is small compared to that on the through-thickness resistivity [11], and (iii) the contact resistivity of the interlaminar interface decreases upon compression in the through-thickness direction [10].

From Eq. (2), the change of the through-thickness resistance of the ith lamina is given by

$$\Delta R_T(i) = \frac{2\Delta\rho_T(i)t(i)}{L_c b}. \quad (6)$$

The change of the through-thickness resistivity $\Delta\rho_T(i)$ of the ith lamina is assumed to be mainly due to the change of the contact resistivity of the interlaminar interface between the ith and $(i-1)$th laminae. In other words, the change in through-thickness volume resistance within lamina i is assumed to be small compared to the change in the contact resistance between laminae i and $i-1$. This assumption is supported by the reported large effects of stress, temperature and humidity on the contact resistivity of the interface between two laminae [10]. An increase of the through-thickness resistivity causes the current penetration to decrease, while a decrease of the through-thickness resistivity causes the current penetration to increase.

Because the contact between adjacent laminae relates to the fiber waviness, which diminishes as the lamina strains in the fiber direction of the lamina, $\Delta\rho_T(i)$ is related to the longitudinal strain of the ith lamina. The more positive is the longitudinal strain, the more positive is $\Delta\rho_T(i)$, since the contact among fibers of adjacent laminae is diminished. The more negative is the longitudinal strain, the more negative is $\Delta\rho_T(i)$, since the contact among fibers of adjacent

laminae is increased. This notion is supported by the observation that the through-thickness resistance increases upon uniaxial tension and decreases upon uniaxial compression [11]. We assume that $\Delta\rho_T(i)$ is proportional to the strain of the ith lamina. Hence

$$\Delta\rho_T(i) = c\varepsilon(i), \tag{7}$$

where c is the proportionality constant and $\varepsilon(i)$ is the longitudinal strain of the ith lamina, as averaged over the span of the beam.

The proportionality constant c can be determined from the experimental results under flexure at the average magnitude of 9.77×10^{-4} for the surface longitudinal strain amplitude (corresponding to a maximum surface longitudinal strain of 1.56×10^{-3}, a maximum deflection of 0.521 mm and a maximum flexural stress of 86.1 MPa) [11]. The fractional change in surface resistance is 0.0911% and 0.0635% for the tension and compression sides, respectively. Substituting these values into Eqs. (1), (3)–(7) yields $c = 9000\ \Omega\,\text{cm}$ for the tension side and $c = 7000\ \Omega\,\text{cm}$ for the compression side.

Under flexure, the distance between the neutral axis and the tension surface is shorter than that between the neutral axis and the compression surface, due to the fact that the compressive modulus is smaller than the tensile modulus. This phenomenon results in the compressive strain at the compressive surface to be larger than the tensile strain at the tensile surface. Instead of considering this difference in strain, this paper considers a difference in c between the tension and compression sides.

The use of experimental results at a particular value of the strain to determine the proportionality constant c is akin to scaling the model to fit reality. Such scaling is limited to a single parameter, i.e., c.

4. Comparison of measured and calculated piezoresistive behavior

The piezoresistivity under flexure is described by the analytical model in Section 2. This section provides a comparison of the calculated and measured [11] piezoresistive behavior, in order to test the effectiveness of the model. For details of the experimental method, please refer to Ref. [11].

Figs. 3–6 show the calculated and experimental results of the fractional change in surface resistance both on the tension side and on the compression side for progressively increasing flexural stress amplitudes (i.e., progressively

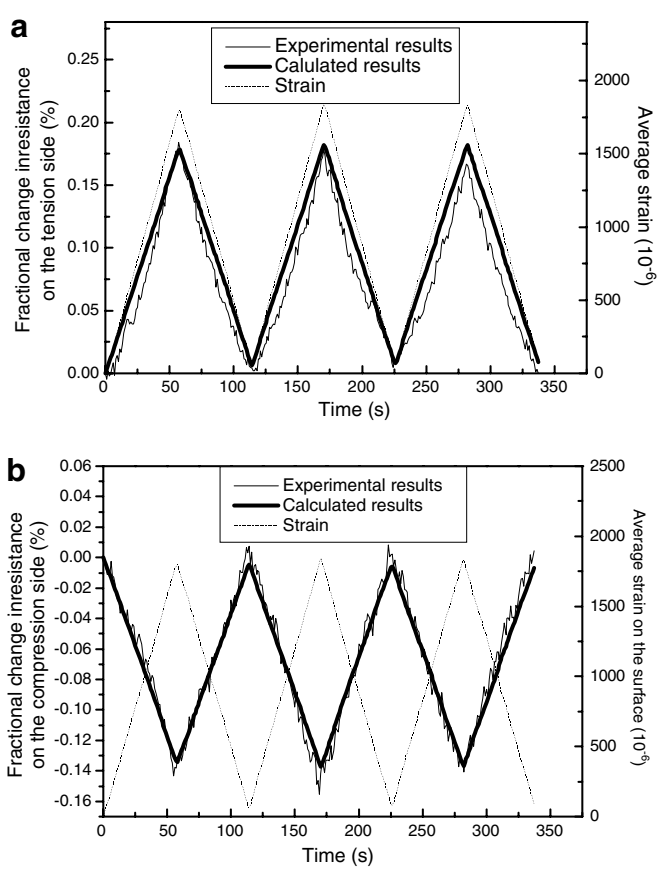

Fig. 3. Comparison of the calculated and measured [11] curves for the change in surface resistance during repeated bending at an amplitude of 1.80×10^{-3} for the average longitudinal strain magnitude at the surface. (a) The tension side. (b) The compression side.

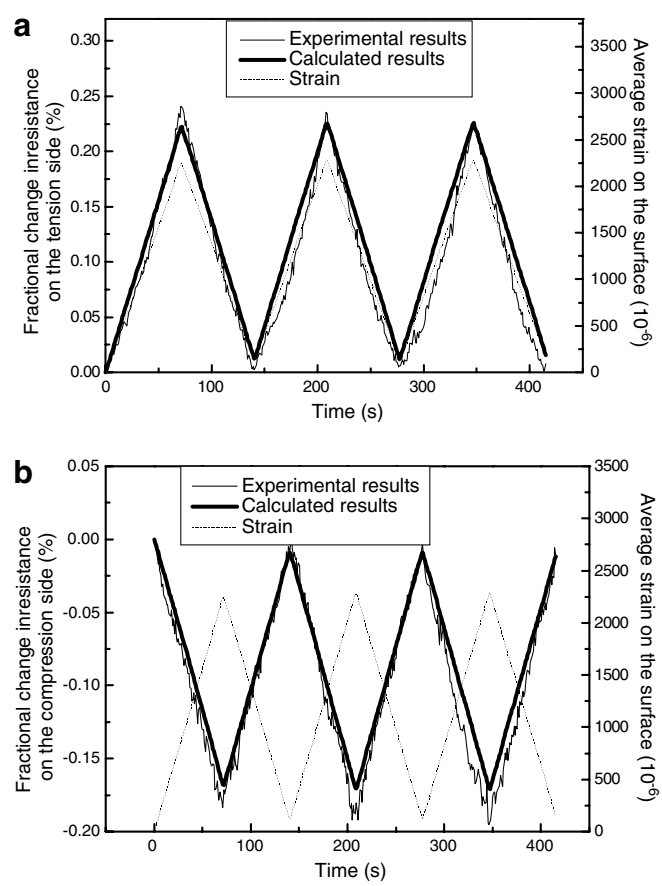

Fig. 4. Comparison of the calculated and measured [11] curves for the change in surface resistance during repeated bending at an amplitude of 2.25×10^{-3} for the average longitudinal strain magnitude at the surface. (a) The tension side. (b) The compression side.

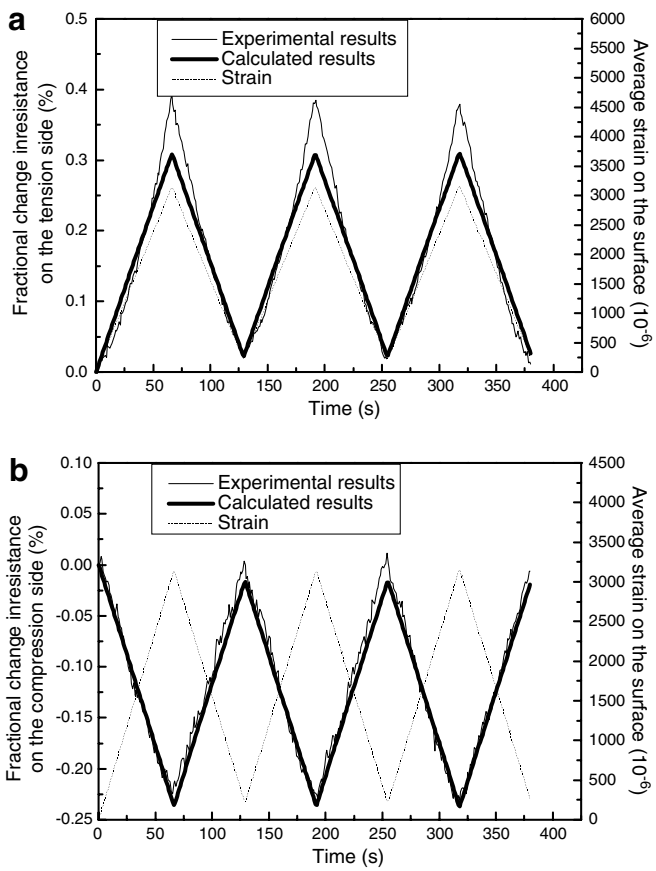

Fig. 5. Comparison of the calculated and measured [11] curves for the change in surface resistance during repeated bending at an amplitude of 3.14×10^{-3} for the average longitudinal strain magnitude at the surface. (a) The tension side. (b) The compression side.

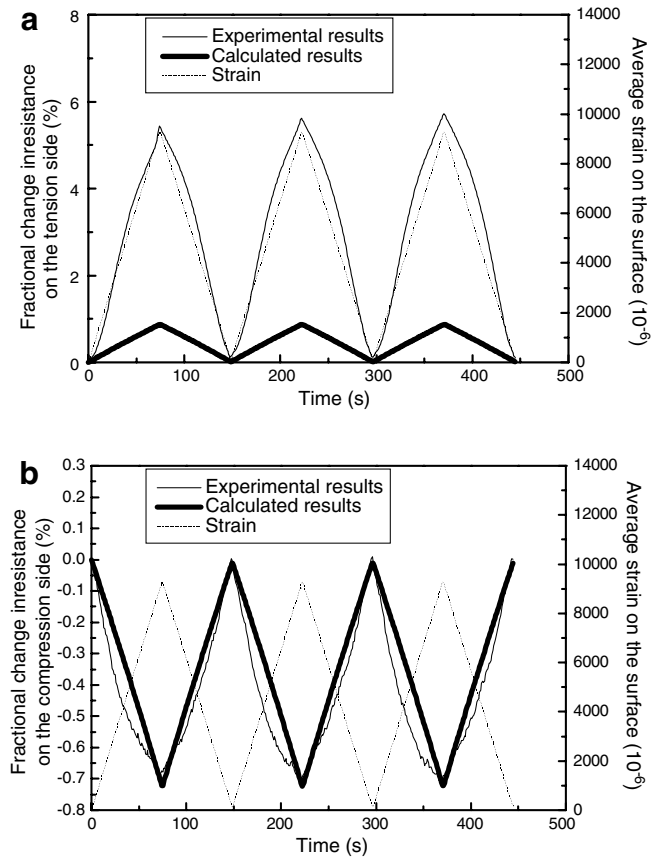

Fig. 6. Comparison of the calculated and measured [11] curves for the change in surface resistance at an average longitudinal strain magnitude of 9.18×10^{-3} at the surface. (a) The tension side. (b) The compression side.

increasing maximum deflection). Excellent agreement was obtained between the calculated and experimental results for the regime of low stress amplitude (Figs. 3 and 4). However, at high stress amplitudes, the calculated values of the fractional change in surface resistance on the tension side are lower than the experimental values (Figs. 5a and 6a), though agreement between the calculated and experimental results remain good on the compression side (Figs. 5b and 6b). This behavior is attributed to minor damage on the tension side, which makes the resistance on the tension side increase much more. This damage is also accompanied by the curves becoming nonlinear (Figs. 6a and b).

Fig. 7 shows the variation of the fractional change in resistance with the maximum average strain (i.e., the average strain on the surface). As noted in relation to Figs. 3–6, agreement between the calculated and experimental values is good for both tension and compression surface resistances, except for the regime of high stress amplitude (i.e., the average longitudinal strain magnitude on the tension/compression surface exceeding 3×10^{-3}). The higher is the stress amplitude, the higher is the measured surface resistance on the tension/compression side compared to the corresponding calculated value, probably due to minor damage. The difference between the measured and calculated results is much larger for the tension side than the compression side.

The plot in Fig. 7 is not meant to show the quantitative relationship between resistance and strain. Rather, it is meant to show that the two quantities indeed correlate with one another, as expected, and more importantly, that the experimental and calculated results are close when the strain is relatively small. We could have used the midspan deflection instead of the average strain on the surface for the horizontal axis, but the latter is scientifically more relevant, particularly since the surface resistance is the quantity in the vertical axis.

The highest stress amplitude used in this work (that in Fig. 6) is 996.2 MPa (corresponding to an average longitudinal strain of 9.18×10^{-3} at the tension surface and a maximum deflection of 4.945 mm) is below the value for failure to occur (1045.1 MPa, corresponding to a maximum deflection of 5.194 mm). The loading in Fig. 6 causes no visible damage [11]. However, minor damage in the form of minor shear between the laminae at the tension surface may occur in Fig. 6, thereby decreasing the current penetration on the tension surface and increasing the surface resistance. This shear between the laminae can be reversible, thereby allowing this shear mechanism to contribute to the reversible change in resistance. Due to geometric constraint, there is

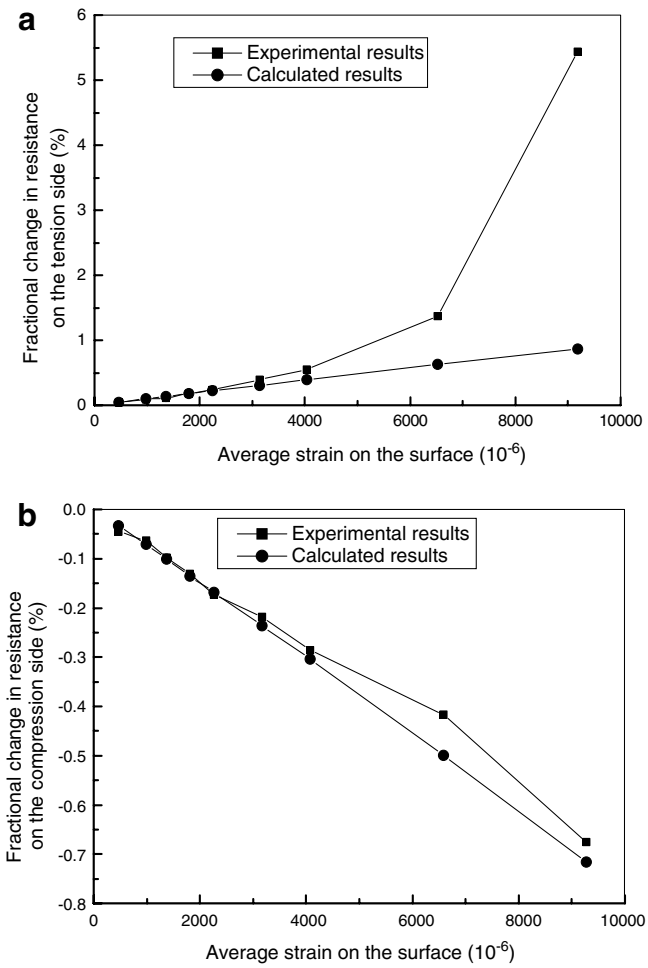

Fig. 7. Comparison of the calculated and measured [11] values of the fractional change in surface resistance at different values of the magnitude of the average longitudinal strain at the surface.

less tendency for such shear deformation to occur at the compression surface. As a result, the difference between the calculated and experimental results in the regime of high strain is much less for the compression surface resistance than the tension surface resistance.

The finding mentioned above means that, in the use of the piezoresistive effect for strain sensing, the compressive surface resistance is a better indicator than the tensile surface resistance. It further means that, in strain sensing, the strain should be limited to low values. The superiority of the compressive surface resistance to the tensile surface resistance is also indicated by the greater linearity of the relationship of the measured resistance with strain, as shown in Figs. 3–5.

5. Conclusion

An analytical model is provided for the piezoresistive phenomenon of continuous carbon fiber polymer–matrix composite under flexure. This phenomenon [11] entails reversible increase of the tension surface resistance and reversible decrease of the compression surface resistance during flexure. The model considers the surface resistance change to be due to change in the degree of current penetration. The longitudinal strain resulting from the flexure affects the through-thickness resistivity, which relates to the contact resistivity of the interlaminar interface, thereby affecting the current penetration. This notion is consistent with the experimental observation that: (i) the through-thickness resistivity decreases upon longitudinal uniaxial tension [9,11,12], (ii) the effect of longitudinal uniaxial tension on the longitudinal volume resistivity is small compared to that on the through-thickness resistivity [11], and (iii) the contact resistivity of the interlaminar interface decreases upon compression in the through-thickness direction [10]. Good agreement is found between the model and prior experimental results [11], except that the calculated surface resistance on the tension side is higher than the measured value when the magnitude of the average longitudinal strain on the surface exceeds 3×10^{-3}.

Acknowledgement

Technical discussion with Dr. Shoukai Wang of University at Buffalo, State University of New York, is gratefully acknowledged.

References

[1] Chung DDL. Self-monitoring structural materials. Mater Sci Eng R 1998;R22(2):57–78.
[2] Wen S, Wang S, Chung DDL. Piezoresistivity in continuous carbon fiber polymer–matrix and cement–matrix composites. J Mater Sci 2000;35(14):3669–75.
[3] Chung DDL, Wang S. Self-sensing of damage and strain in carbon fiber polymer–matrix structural composites by electrical resistance measurement. Polym Polym Compos 2003;11(7):515–25.
[4] Angelidis N, Wei CY, Irving PE. The electrical resistance response of continuous carbon fibre composite laminates to mechanical strain. Compos: Part A 2004;35:1135–47.
[5] Wen S, Chung DDL. Self-sensing of flexural damage and strain in carbon fiber reinforced cement and effect of embedded steel reinforcing bars. Carbon 2006;44(8):1496–502.
[6] Wen S, Chung DDL. Effects of strain and damage on the strain sensing ability of carbon fiber cement. J Mater Civil Eng 2006;18(3):355–60.
[7] Wen S, Chung DDL. Strain sensing characteristics of carbon fiber reinforced cement. ACI Mater J 2005;102(4):244–8.
[8] Wang S, Chung DDL. Self-monitoring of strain and damage by a carbon–carbon composite. Carbon 1997;35(5):621–30.
[9] Wang X, Chung DDL. Continuous carbon fiber epoxy–matrix composite as a sensor of its own strain. Smart Mater Struct 1996;5(6):796–800.
[10] Wang S, Kowalik DP, Chung DDL. Self-sensing attained in carbon fiber polymer–matrix structural composites by using the interlaminar interface as a sensor. Smart Mater Struct 2004;13(3):570–92.
[11] Wang S, Chung DDL. Self-sensing of flexural strain and damage in carbon fiber polymer–matrix composite by electrical resistance measurement. Carbon 2006;44(13):2739–51.
[12] Wang X, Fu X, Chung DDL. Electromechanical study of carbon fiber composites. J Mater Res 1998;13(11):3081–92.
[13] Xiao J, Li Y, Fan X. A laminate theory of piezoresistance for composite laminates. Compos Sci Technol 1999;59(9):1369–73.

[14] Kupke M, Schulte K, Schüler R. Non-destructive testing of FRP by D.C. and A.C. electrical methods. Compos Sci Technol 2001;61: 837–47.
[15] Abry JC, Choi YK, Chateauminois A, Dalloz B, Giraud G, Salvia M. In-situ monitoring of damage in CFRP laminates by means of AC and DC measurements. Compos Sci Technol 2001;61(6):855–64.
[16] Wang X, Chung DDL. Fiber breakage in polymer–matrix composite during static and dynamic loading, studied by electrical resistance measurement. J Mater Res 1999;14(11):4224–9.
[17] Wang X, Wang S, Chung DDL. Sensing damage in carbon fiber and its polymer–matrix and carbon–matrix composites by electrical resistance measurement. J Mater Sci 1999;34(11):2703–14.
[18] Chu Y-W, Yum Y-J. Detection of delamination in graphite/epoxy composite by electric potential method. In: Proceedings – KORUS 2001, the 5th Korea–Russia international symposium on science and technology, Section 5 – Mechanics and Automotive Engineering, 2001. p. 240–2.
[19] Irving PE, Thiagarajan C. Fatigue damage characterization in carbon fibre composite materials using an electrical potential technique. Smart Mater Struct 1998;7:456–66.
[20] Ceysson O, Salvia M, Vincent L. Damage mechanisms characterization of carbon fibre/epoxy composite laminates by both electrical resistance measurements and acoustic emission analysis. Scripta Mater 1996;34(8):1273–80.
[21] Kaddour AS, Al-Salehi AR, Al-Hassani STS, Hinton MJ. Electrical resistance measurement technique for detecting failure in CFRP materials at high strain rates. Compos Sci Technol 1994;51(3):377–85.
[22] Wang S, Chung DDL, Chung JH. Impact damage of carbon fiber polymer–matrix composites, monitored by electrical resistance measurement. Compos. Part A – Appl. S. 2005;36:1707–15.
[23] Masson LC, Irving PE. Comparison of experimental and simulation studies of location of impact damage in polymer–matrix composites using electrical potential techniques. In: Gobin PF, Friend CM, editors. Proc. SPIE fifth European conference on smart structures and materials, vol. 4073; 2000. p. 182–93.
[24] Angelidis N, Khemiri N, Irving PE. Experimental and finite element study of the electrical potential technique for damage detection in CFRP laminates. Smart Mater Struct 2005;14:147–54.
[25] Wang S, Chung DDL, Chung JH. Self-sensing of damage in carbon fiber polymer–matrix composite by measuring the electrical resistance or potential away from the damaged region. J Mater Sci 2005;40: 6463–72.
[26] Wang X, Chung DDL. An electromechanical study of the transverse behavior of carbon fiber polymer–matrix composite. Compos Interface 1998;5(3):191–9.